

# Investigations of a Control Surface Seal for Reentry Vehicles

Patrick H. Dunlap Jr.\* and Bruce M. Steinetz†

*NASA John H. Glenn Research Center at Lewis Field, Cleveland, Ohio 44135*

Donald M. Curry‡

*NASA Johnson Space Center, Houston, Texas 77058*

Jeffrey J. DeMange§

*University of Toledo, Toledo, Ohio 43606*

H. Kevin Rivers¶

*NASA Langley Research Center, Hampton, Virginia 23681*

and

Su-Yuen Hsu\*\*

*Lockheed Martin Space Operations, Hampton, Virginia 23681*

Reentry vehicles generally require control surfaces such as rudders and body flaps to steer them during flight. Control surface seals are installed along hinge lines and where control surface edges move close to the vehicle body. These seals must operate at high temperatures and limit heat transfer to underlying structures to prevent overheating and possible loss of vehicle structural integrity. Test results are presented for the baseline rudder/fin seal design for the X-38 reentry vehicle. Compressing seals at the predicted peak seal temperature of 1900°F resulted in loss of seal resiliency. The vertical Inconel rudder/fin rub surface was redesigned to account for this loss of resiliency. Room-temperature compression tests revealed that seal unit loads and contact pressures were below limits set to protect shuttle thermal tiles on the horizontal sealing surface. The seals survived an ambient-temperature 1000 cycle scrub test over sanded shuttle tiles and were able to disengage and reengage the tile edges during testing. Arcjet tests on a single seal caused a large temperature drop ( $\Delta T = 1710^\circ\text{F}$ ) in the seal gap and confirmed the need for seals in the rudder/fin gap location. These test results verified that this seal is satisfactory for the X-38 application.

## Nomenclature

$A$	=	frontal area of seal exposed to flow, $\text{ft}^2$
$K$	=	seal permeability, $\text{ft}^2$
$L$	=	length of flow path through seal, ft
$\dot{m}$	=	flow through seal, $\text{lbm/s}$
$V_{\text{covered seal}}$	=	volume of alcohol displaced by seal covered with plastic wrap, ml
$V_f$	=	seal fiber volume ratio
$V_i$	=	individual seal component volumes, $\text{in}^3$
$V_{\text{plastic wrap}}$	=	volume of alcohol displaced by plastic wrap, ml
$V_{\text{total}}$	=	total seal volume, $\text{in}^3$
$V_{\text{uncovered seal}}$	=	volume of alcohol displaced by uncovered seal, ml
$\Delta P$	=	pressure drop across seal, $\text{lbf/ft}^2$
$\Delta T$	=	temperature drop across seal location, $^\circ\text{F}$
$\varepsilon$	=	seal porosity
$\mu$	=	dynamic viscosity of air, $3.86 \times 10^{-7} \text{ lbf} \cdot \text{s/ft}^2$
$\rho$	=	density of air at 300 K, $0.0768 \text{ lbm/ft}^3$

Presented as Paper 2002-3941 at the 38th Joint Propulsion Conference, Indianapolis, IN, 7–10 July 2002; received 20 August 2002; revision received 5 March 2003; accepted for publication 13 March 2003. This material is declared a work of the U.S. Government and is not subject to copyright protection in the United States. Copies of this paper may be made for personal or internal use, on condition that the copier pay the \$10.00 per-copy fee to the Copyright Clearance Center, Inc., 222 Rosewood Drive, Danvers, MA 01923; include the code 0022-4650/03 \$10.00 in correspondence with the CCC.

\*Mechanical Engineer, Mechanical Components Branch. Member AIAA.  
†Senior Research Engineer, Mechanical Components Branch. Member AIAA.

‡Aerospace Technologist, Thermal Branch.

§Senior Research Associate, Mechanical Components Branch. Member AIAA.

¶Aerospace Engineer, Metals and Thermal Structures Branch.

\*\*Aeronautical Engineer, Supporting Metals and Thermal Structures Branch.

## Introduction

SINCE the space shuttle went into regular service in 1981, NASA has been examining vehicle concepts both to complement and replace this launch system. Vehicles capable of putting payloads and personnel into orbit with faster turnaround times, with higher safety margins, and at lower costs are especially in demand now that the International Space Station (ISS) is in orbit. New vehicle concepts are being pursued for crew transfer vehicles, such as the X-37, and crew return vehicles (CRVs), such as the X-38, that would be used to transport personnel while in orbit or to leave the space station during a medical emergency or an evacuation.

Although each vehicle concept is unique, they all have some combination of control surfaces that steer or guide the vehicles during reentry into and through the Earth's atmosphere. These control surfaces include rudders, body flaps, elevons, and other surfaces that move with respect to the body of the vehicle. Seal interfaces exist between these movable surfaces and stationary portions of the vehicle both along hinge lines and where control surface edges seal against the vehicle body. These seals must operate in high-temperature environments and limit hot-gas ingestion and transfer of heat to underlying low-temperature structures to prevent overtemperature of these structures and possible loss of the vehicle. Hinge line seals are especially important because they ensure that the actuators that move the control surfaces remain cool enough to operate and control the flight of the vehicle.

One recent vehicle concept is the X-38 vehicle that NASA designed to demonstrate technologies that would be required for a potential CRV for the ISS (Fig. 1). The vehicle is designed to glide from orbit in an unpowered freefall that is controlled by two movable rudders, two body flaps located at the aft end of the vehicle, and a steerable parafoil deployed after reentry. Seal interfaces exist between the movable body flaps and the bottom surface of the vehicle and between the rudders and their respective fins (Fig. 1). Wong and Kremer<sup>1</sup> performed a series of two-dimensional computational fluid dynamics studies that modeled the gap between the

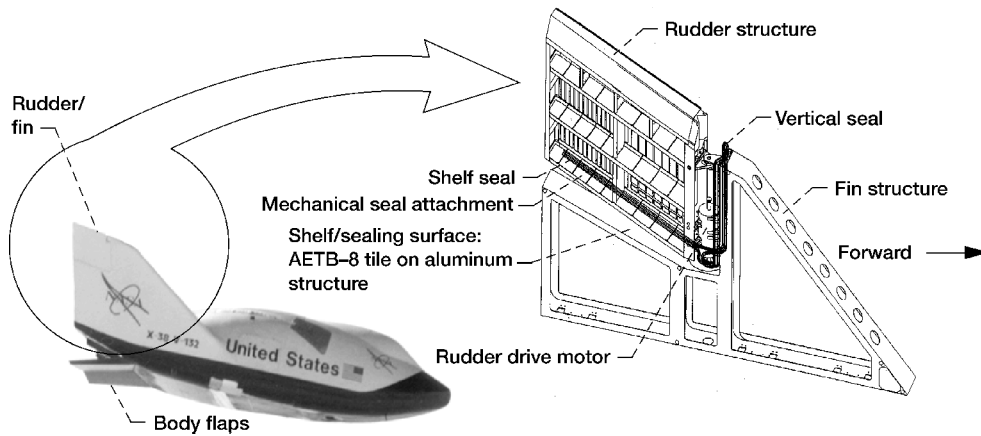


Fig. 1 X-38 vehicle and rudder/fin structure and seal locations.

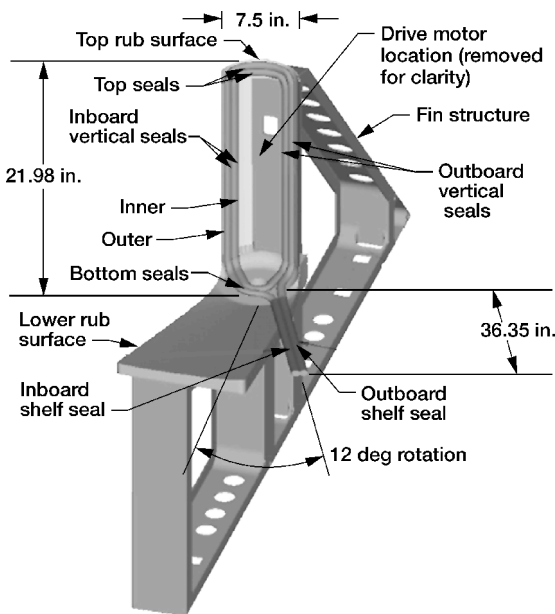


Fig. 2 Computer model depicting rudder/fin seal rotated to full outboard position with seal dimensions.

rudder and fin during reentry of the X-38 vehicle and concluded that a seal is required along this interface to prevent excessive local heat fluxes on these structures.

The objectives of the current study were to summarize the tests and analyses that have been performed on the baseline seal design for the X-38 rudder/fin seal and assess the seal's capabilities relative to future reusable launch vehicle requirements. The specific goals of this effort were as follows. The first goal was to measure seal flow rates, resiliency, and unit loads both in an as-received condition and after temperature exposure. The second goal was to examine seal durability and wear resistance to recommend rub-surface treatments required to maximize seal wear life. The third goal was to determine the effects of seal damage incurred during scrubbing on flow rates through the seals. The final goal was to determine experimentally anticipated seal temperatures for representative external flow boundary conditions under arcjet test conditions simulating vehicle reentry.

### Case Study: Design Requirements for X-38 Rudder/Fin Seal System

The design of the X-38 rudder/fin seal assembly consists of a double seal attached to the rudder that seals the vertical hinge line and the fin shelf line (Figs. 1 and 2). The vertical seal loop surrounds and protects the rudder drive motor and attachments between the rudder and the fin (Fig. 2). The seal assembly must allow the rudder

to rotate during the entire mission and must accommodate a rotation range of  $\pm 12$  deg (Fig. 2).

### Temperature Limits/Temperature Drop

The rudder/fin seal assembly will be expected to endure high temperatures caused by convective heating in an oxidative environment with radiation exchange in the seal gap. A thermal analysis predicted that peak temperatures for the exposed seal could reach from approximately 1900°F (with laminar boundary-layer assumption) to 2100°F (with turbulent boundary-layer assumption) with seal attachment temperatures of 1500°F (Fig. 3). Peak temperatures occur about 1200 s (20 min) into reentry with a subsequent decrease in temperatures for the remainder of the reentry. Materials used in the seals must be able to withstand these high temperatures. Because the predicted attachment temperature exceeds current adhesive temperature limits, the seals must be mechanically attached to the seal carrier plate and rudder. In addition to withstanding these extreme temperatures, the seals must act as a thermal barrier to minimize temperature increases downstream of the seal to protect underlying low-temperature structures. In particular, the electromechanical actuators used to move the rudders must be kept cool enough for them to operate properly. A detailed discussion of the thermal analysis will be given later in the paper in the "Thermal Analysis" section.

### Pressure Drop

The maximum predicted pressure drop across the seal during vehicle reentry is about 56 lbf/ft<sup>2</sup> (psf, outboard, high pressure) and occurs about 450 s after the peak heating (Fig. 3). To be conservative, flow tests were conducted up to the peak pressure. The pressure across the seal during peak heating is 35 psf and occurs at about 1200 s into the reentry mission (Fig. 3).

### Resiliency

No specific design requirement was established for seal resiliency. A main requirement for the seals is that they remain in contact with the sealing surface while the vehicle goes through the maximum reentry heating cycle. The seals must be able to accommodate differences in thermal expansion between parts adjacent to them that cause the seal gap to change size. Subsequent to the reentry heating cycle, any small thermally induced gap opening is of no consequence because the convective heating rate drops off sharply.

### Seal Loads/Gap

The seals are to be installed at approximately 20% compression to ensure good sealing contact with the rudder/fin surfaces (Fig. 4). The seals will seal against shuttle-derived tile that limits the maximum seal unit or contact load. The tiles used for the rudder/fin horizontal shelf sealing surface are alumina enhanced thermal barrier, 8-lb/ft<sup>3</sup> density (AETB-8) with reaction cured glass (RCG)/toughened uni-piece fibrous insulation (TUFI) coating. Designers have set a unit load limit of less than 5 lb/in. of seal to prevent tile damage during

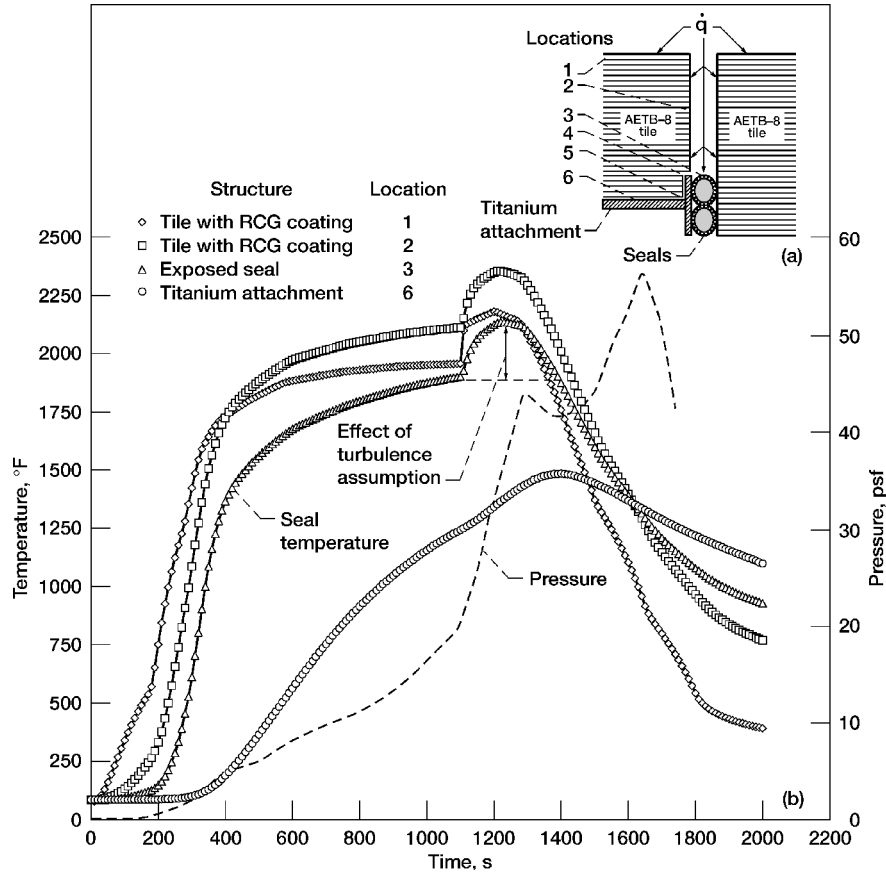


Fig. 3 Thermal analysis of rudder/fin seal: a) rudder/fin gap area TMM and b) rudder/fin seal temperature and pressure predictions.

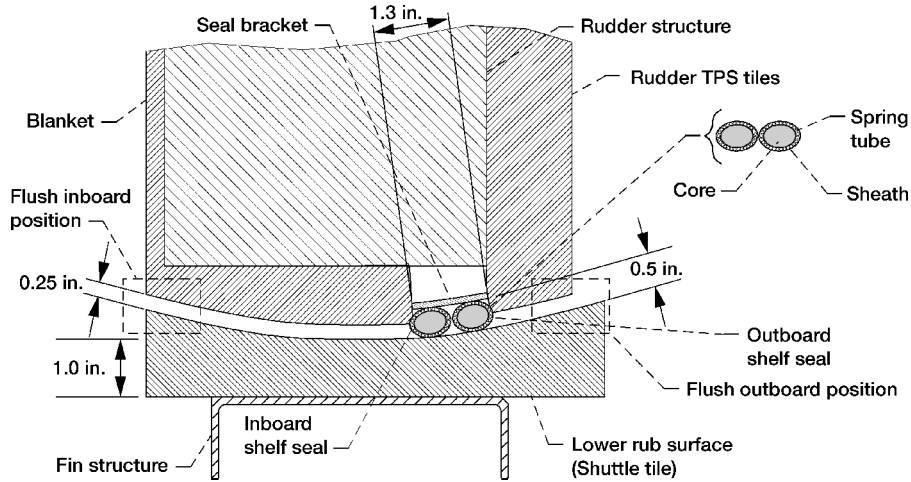


Fig. 4 Cross section of rudder/fin shelf seal location (standing aft looking forward) showing seal components.

installation or actuation. The seals are required to seal a nominal 0.25-in. gap between the surfaces of the X-38 rudder and fin.

**Life/Wear Resistance**

The X-38 rudder/fin seals are only required to last for one mission and will subsequently be replaced after each mission. The seals must be robust enough to endure the scrubbing that they will experience during preflight checkouts and during the mission. The vertical hinge line seals are scrubbed over an Inconel sealing surface as the rudder actuates, but they are designed to remain in contact with that surface throughout the mission. The rudder/fin shelf seals experience both scrubbing against the AETB-8 tiles and a “scissoring” action as they are moved onto and off of the shelf sealing surface. When the seals are moved off of the fin shelf, they will tend to return to

an uncompressed shape. As they are moved back onto the surface and compressed again, they must be able to endure the shear forces that they will be subjected to without causing excessive loads on the rudder drive motor. Because the rudder/fin shelf seals will be exposed to more severe loading conditions, the wear resistance of these seals is examined as part of the current study.

**Test Apparatus and Procedures**

**Seal Specimens**

The seal design examined in this study had a nominal diameter of 0.62 in., where  $1 \times 10^{-3}$  in. = 25  $\mu$ m (Table 1 and Fig. 4). Seals consisted of an Inconel X-750 spring tube stuffed with Saf-fil batting and overbraided with two layers of Nextel 312 ceramic fibers. The Saf-fil batting stuffed into the Inconel spring tube had

**Table 1** X-38 seal construction matrix

Characteristic	Property
Diameter, in.	0.620
Core	
Material	Saffil
Density, lb/ft <sup>3</sup>	6
Measured % of seal by mass	12.5
Spring tube	
Material	Inconel X-750
Measured % of seal by mass	33
Sheath	
Material	Nextel 312 fabric
No. of layers	2
Measured % of seal by mass	54.5

an overall density of 6 lb/ft<sup>3</sup>. The density of each individual Saffil filament was 0.0975 lb/in.<sup>3</sup> (2.70 g/cm<sup>3</sup>). The Nextel 312 fabric was a 3M product composed of 62% Al<sub>2</sub>O<sub>3</sub>, 24% SiO<sub>2</sub>, and 14% B<sub>2</sub>O<sub>3</sub>. The density of the individual ceramic fibers in this fabric was 0.123 lb/in.<sup>3</sup> (3.4 g/cm<sup>3</sup>). The density of the Inconel X-750 wire used in the spring tube was 0.298 lb/in.<sup>3</sup> (8.25 g/cm<sup>3</sup>). This seal design will hereafter be referred to as the 6-pcf (pounds per cubic foot) design. The seal is currently used in several places on the Space Shuttle Orbiters including the main landing gear doors, the orbiter external tank umbilical door, and the payload bay door vents. It was selected as the baseline seal design for the rudder/fin location of the X-38.

#### Thermal Analysis

An analysis was performed on the X-38 rudder/fin seal location to predict maximum seal and attachment temperatures during vehicle reentry. Figure 3 shows a schematic of the rudder/fin gap area thermal math model (TMM) and predicted temperatures for the exposed seal and surrounding hardware. The TMM was a quasi-two-dimensional representation built using SINDA version 3.1. The model consisted of approximately 150 nodes that represented the thermal protection system (TPS) tiles, the dual seals, and the titanium attachment structure (Fig. 3a). The TPS material on both the rudder and the fin was modeled as RCG/TUFI-coated AETB-8 tile. The seal was modeled as Nextel 312 fabric over Saffil batting (6 lb/ft<sup>3</sup>). The seal attachment was modeled as a solid titanium structure. For each material, temperature-dependent and pressure-dependent (where required) properties were used. All connections between dissimilar materials were assumed to be perfect, that is, no contact resistance was modeled. The gap was modeled as being 1.5 in. deep and 0.25 in. wide. All modes of heat transfer including conduction, convection, and radiation were accounted for in the model. The model did not include the effects of flow through the seal. The Thermal Synthesizer System (TSS) was used to resolve the radiation exchange between all exposed surfaces inside and outside of the gap, including radiation to space. Results from the TSS analysis were coupled to the SINDA analysis program.

The surface heating used to drive the TMM was based on cycle 8 reference heating supplied by Winston Goodrich of the Johnson Space Center Aeroscience and Flight Mechanics Division. The heating supplied was representative of the heating predicted on the windward surface of the rudder/fin area. The heating distribution within the gap was determined using the gap heating relationship presented by Nestler.<sup>2</sup> Nestler's empirical relationship provides for the heat flux to a certain gap depth, for example, to the seal, and assumes no flow through the floor of the gap as would occur for an impermeable seal.

#### Temperature Exposure Tests

The thermal analysis predicted that the rudder/fin seals would be exposed to temperatures at or above 1900°F during X-38 reentry. To simulate exposure to such extreme temperatures and to determine the effects that this exposure has on the seals, specimens were placed into a tube furnace in a compressed state and heated at 1900°F for 7 min. This 7-min temperature exposure closely simulated the amount of time that the seals would spend at the peak temperature during reentry (Fig. 3b).

In these tests, 1-ft-long seal specimens were clamped into a fixture between two flat stainless steel plates and subjected to a linear compression of 20, 25, or 30% of their overall diameter of 0.62 in. After temperature exposure, the fixture and specimen were removed from the furnace and allowed to cool at room temperature. Specimens were then removed from the test fixture and subjected to compression tests to examine the effects that the temperature exposure had on the stiffness and resiliency of these seals. Further details of the setup and procedure for these temperature exposures can be found in the paper by Dunlap et al.<sup>3</sup>

#### Porosity Measurements

Seal porosity was measured using two different approaches.

##### Archimedes Approach

The first approach was based on Archimedes's theory of volume displacement. This principle states that the volume of liquid that is displaced when a solid object is dropped into the liquid is equal to the volume of the solid. Seal porosity was determined by putting covered and uncovered seal specimens into a 100-ml graduated cylinder partially filled with isopropyl alcohol and comparing the volume displaced by the specimen in each condition. A total of four seal specimens of approximately 2.5–3 in. in length were tested. For each measurement, a seal specimen was wrapped in plastic wrap and dropped into the graduated cylinder. Covering the specimens in plastic wrap prevented alcohol from penetrating into the porous structure of the seal and allowed the cylindrical volume of the exterior of the seal to be determined. The volume level of the alcohol in the cylinder was measured before and after the seal was inserted so that the difference in volume was the amount displaced by the seal. The specimen was then taken out of the cylinder, and the plastic wrap was removed from it. The wrap was then placed into the cylinder by itself to determine how much volume it displaced. This amount was subtracted from the volume measured for the wrapped seal to determine the actual volume that only the exterior of the seal would have displaced. Finally the unwrapped specimen was placed into the cylinder. Alcohol easily soaked into the uncovered seals and filled the voids inside of them. After allowing the alcohol to absorb into the seal, the volume displaced by the material in the seal was recorded. Porosity was then calculated as

$$\varepsilon = 1 - V_f = 1 - \left( \frac{V_{\text{uncovered seal}}}{V_{\text{covered seal}} - V_{\text{plastic wrap}}} \right) \quad (1)$$

##### Mass/Volume Approach

A mass/volume technique for determining seal porosity was used to corroborate the results of the Archimedes approach. First, overall specimen volume was determined by making precision measurements of the cross-sectional dimensions of the ends of 1-in.-long seal specimens compressed in a groove machined in a test block. A flat plate compressed the seal in the groove to the 20% design compression. The total volume was determined by multiplying the measured seal elliptical cross-sectional area times the seal length. Next, the seal was cut open and separated into its individual components: the Saffil core, Inconel spring tube, and Nextel sheath. Each of these constituents was weighed on a precision (1-mg) mass balance to determine its respective mass. Volumes of each of the constituents were then determined by dividing their masses by their respective individual fiber densities. Finally the fiber volume ratio was found by summing the individual constituent volumes and dividing by the total measured volume. Porosity was determined for the two specimens as

$$\varepsilon = 1 - V_f = 1 - \left( \frac{\sum V_i}{V_{\text{total}}} \right) \quad (2)$$

#### Compression Tests

##### Test Fixture

Compression tests were performed to determine seal preload and resiliency behavior at room temperature using a precision linear-slide compression test fixture. A specimen was loaded into

a stationary grooved specimen holder, and an opposing plate was compressed against the specimen. The groove was rectangular in shape with a width of 0.62 in. and a depth of 0.37 in. Stainless-steel shims were placed in the groove behind the specimen to vary the amount of compression on the seal. The amount of compressive load on the specimen was measured vs the amount of linear compression for several load cycles. Multiple load cycles were applied to the specimen before the preload data set was recorded to remove the effects of hysteresis and permanent set that accumulated with load cycling of the specimens. Most permanent set occurred within the first four load cycles, so four load cycles were performed for each test. A pressure-sensitive film mounted on the opposing plate was used to determine the contact width of the specimen as it was compressively loaded. The footprint length and width at the end of the fourth load cycle were used to calculate seal preload in pounds per square inch. The measured load vs compression data was used to determine residual interference corresponding to a given linear crush value.<sup>4</sup> Residual interference is defined as the distance that the specimen will spring back while maintaining a load of at least 0.01 lb/in. of specimen. The hardware and procedure used to perform these tests are described in detail by Steinetz et al.<sup>4</sup> Overall accuracy of the preload values measured using this method was calculated to be  $\pm 3.4\%$  (Ref. 5).

#### Test Matrix

In previous studies by Dunlap et al.,<sup>3,6</sup> seal compression tests were performed at compression levels of 10, 20, 25, and 30% of the specimen's as-received overall diameter. Control surface seals are typically installed at approximately 20% compression, including the seals used in the X-38 rudder/fin seal application. Tests carried out at the low-compression level of 10% compression were performed to determine seal resiliency and preload under minimal loading conditions. The low-compression tests were performed to simulate conditions in which seals may become unloaded during use or take on a large permanent set due to temperature exposure. Tests were also performed on seal specimens after temperature exposure. Primary and repeat compression tests were performed for all test conditions.

#### Scrub/Wear Tests

To test seal wear resistance, a series of tests were performed in which the seals were scrubbed over a representative sealing surface for repeated cycles. These tests also examined the structural integrity of the seal attachment technique and the ability of the seals to engage and disengage the shelf sealing surface while the rudder pivoted through its  $\pm 12$  deg of rotation.

#### Test Fixture

The seals were evaluated in a test fixture that simulated the motion of the X-38 rudder with respect to a stationary sealing surface such

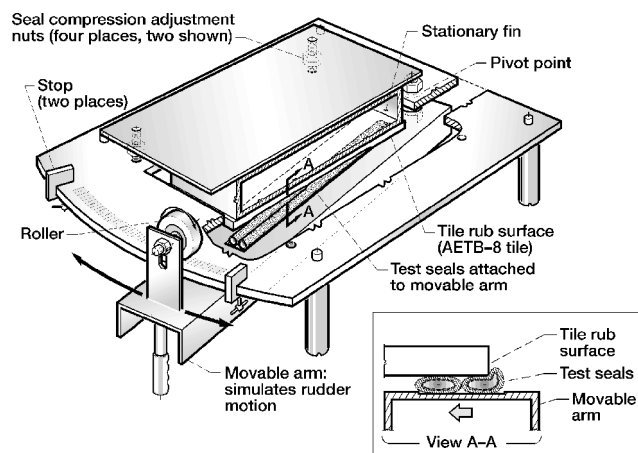


**Fig. 5** Isometric of scrub/wear test fixture showing seals reengaging the tile rub surface.

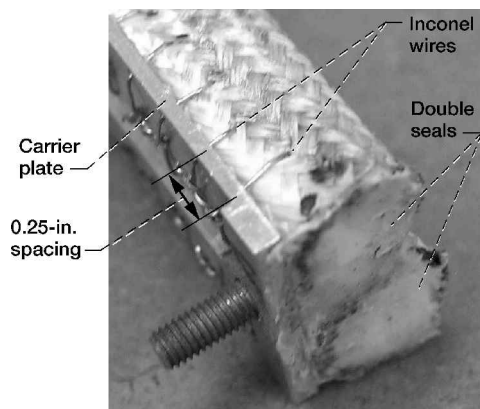


**Fig. 6** Photograph of double seals mechanically attached to carrier plate with Inconel wires for scrub testing.

as the fin shelf (Fig. 5). In these tests, two seals were mechanically attached side-by-side to a representative carrier plate by threading 0.020-in.-diam Inconel 600 annealed (MS20995N20) wires through the outer layers of the bottom of the seal, passing the ends of the wires through holes in the plate, and twisting the wire ends to secure the seals (Fig. 6). These loops of wire were located every 0.25 in. along the carrier plate. Two different seal lengths were tested due to a limited supply of seal material: a full-scale seal that was 27.5 in. long and a shorter 6.5-in. seal. A coating of vermiculite (Microlite Vermiculite Dispersions, 923, from W. R. Grace and Company) was brushed on the seals. This treatment has been shown to prevent fraying and reduce abrasion of fabrics. For each test, the seal/carrier plate assembly was attached to the top surface of a movable arm that simulated the rudder in the rudder/fin seal assembly (Figs. 2 and 4). The movable arm was pivoted on one end and mounted on the underside of a table (Fig. 5). At the other end of the arm was a roller that allowed the arm to be suspended below the table and to rotate freely with respect to the pivot. Two stops fixed to the edge of the table limited the amount of rotation of the arm to  $\pm 12$  deg. The seals were scrubbed against a simulated seal rub surface that was suspended through a rectangular hole cut in the center of the table. Four bolts and adjustment nuts were used to compress the rub surface against the test seals to the design point of 20% compression.

The rub surface used for these tests was composed of three RCG/TUFI coated AETB-8 tiles. The three tiles were lined up side-by-side opposite the seals along the length of the movable arm. The total length of these tiles was identical to the length of the fin shelf sealing surface on the X-38 rudder/fin. Gap fillers consisting of four-ply planar Nextel 312 sleeving about 0.10 in. thick were bonded into the joints between the tiles. Assembly of the scrub test fixture revealed the need for the gap fillers to be installed flush with the outer surface of the tiles to minimize sneak flows between adjacent tiles above the gap fillers. The 27.5-in. seal was scrubbed against all three tiles with gap fillers between the tiles. Based on the results of this first test in which damage was observed in areas where the seal was scrubbed over joints between the tiles, the 6.5-in. seal was installed for the second test such that the center portion of the seal passed over a tile joint. In addition, Kapton<sup>®</sup> tape was placed over the gap between the tiles to see if smoothing that area would reduce the amount of damage the seals incurred during scrubbing. With use of a profilometer, the surface roughness of the sanded tiles in areas away from the joints was measured at 80–90  $\mu$  in. rms before testing.

#### Test Procedure

During a test, the arm was manually rotated back and forth from one stop to the other over the full range of  $\pm 12$  deg. Each rub surface was sized so that the seals would move off of the edges of the surface and out of contact with it as the arm was moved between the stops in both directions. This forced the seals to reengage the rub surface as the arm rotated back toward the centerline of the rub surface (see view A-A in Fig. 5). A 0.25 in. radius was fashioned into the tile edges to ease reengagement of the seals back onto the tile surface.

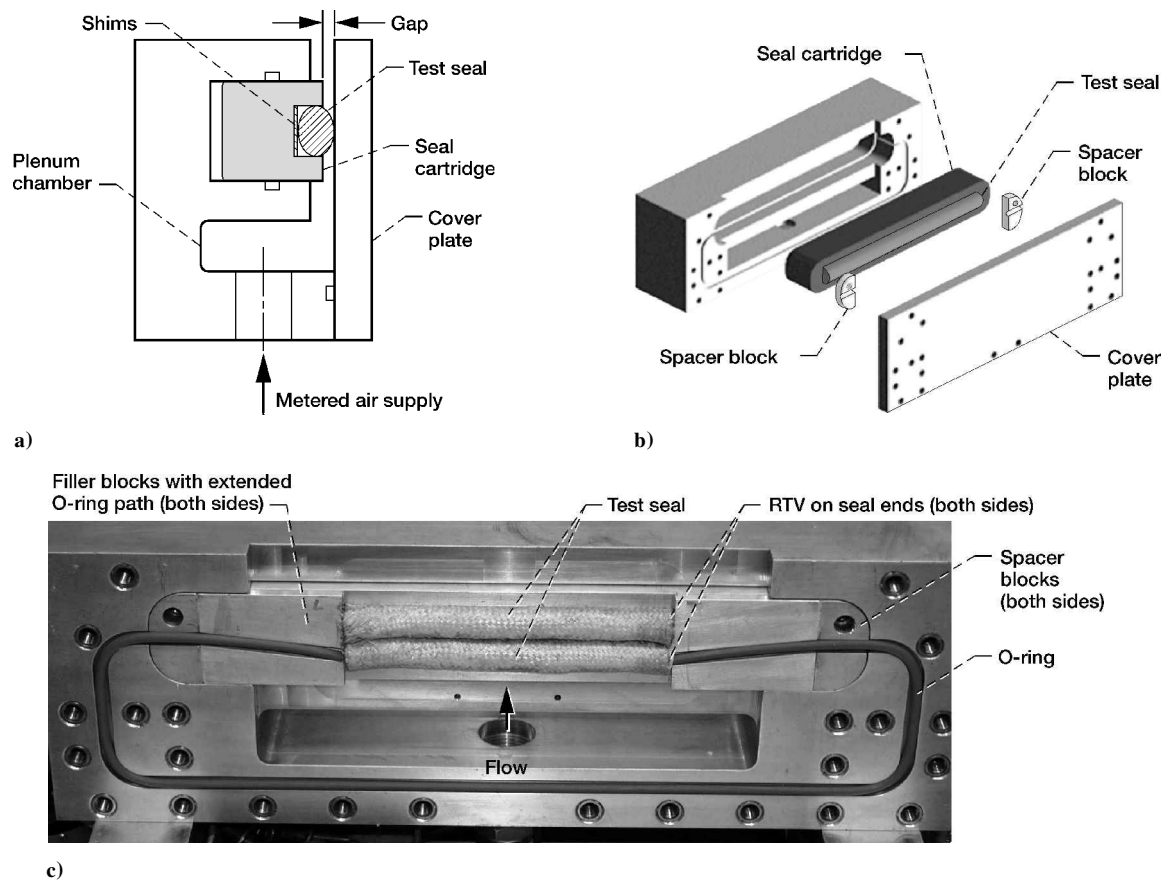


Fig. 7 Schematic of flow fixture: a) cross section, b) isometric, and c) front view of 6.5-in. seal specimen installed in flow fixture showing grooved filler blocks that join O-ring to both ends of seal.

A torque meter located at the pivot point measured the amount of torque required to rotate the arm and scrub the seals over the rub surface. The torque meter was also used to measure the amount of torque required to engage and disengage the seals as they were moved off of and back onto the rub surface. Both test seals were subjected to 1000 scrub cycles. This cycle count was selected as a conservative estimate of the number of cycles the seals would experience during preflight checkout and during the single mission.

#### Flow Tests

Flow tests were performed on the seals in an ambient-temperature linear flow fixture shown schematically in Fig. 7. The flow fixture was designed so that either single or double seals of different diameters could be tested in removable cartridges that are inserted into the main body of the test fixture. Seals can be tested in this fixture with different seal gaps and under different amounts of linear compression.

#### Flowpath/Instrumentation

During flow testing, pressurized air entered through an opening in the base of the fixture and passed through a plenum chamber before reaching the test seal. Air flowed through the gap between the cartridge and the cover plate, passed through the seal and its interface with the cover plate, and then flowed out of the top of the fixture (Fig. 7a). A flow meter upstream of the flow fixture measured the amount of flow that passed through the test seal. The flow meter had a range of 0–100 standard l/min ( $0-4.5 \times 10^{-3}$  lbm/s) and an accuracy of 1% of full scale. A pressure transducer (0–5 psi differential, 0.07% accuracy) upstream of the test seal measured the differential pressure across the seal with respect to ambient conditions, and a thermocouple measured the upstream temperature.

#### Test Fixture

Test seals were mounted in the groove of a test cartridge (Fig. 7b). Individual cartridges were machined with a groove width for a sin-

gle seal of 0.62 in. and a groove width for a double seal of 1.30 in. Two different seal lengths were used in this series of tests. Seals that had been scrub tested were approximately 6.5 in. long, whereas as-received seals that had not been scrubbed were tested in either 6.5 or 12 in. lengths. For the 12-in. seals, the amount of preload, or linear compression, was varied by placing steel shims in the cartridge groove behind the seal. A slightly different setup was used for the 6.5-in. seals (Fig. 7c). These seals were mechanically attached to carrier plates, and the entire assembly of the seal and carrier plate was installed in the center of the 12-in.-long groove of the test cartridge. Aluminum blocks with O-ring grooves in them were installed on either side of the seal assembly to seal the outboard seal ends.

After a seal specimen was installed in the cartridge, the cartridge was inserted into the test fixture. An O-ring sealed the perimeter of the cartridge chamber to prevent flow from passing behind the cartridge during testing. Pairs of spacer blocks secured to the cartridge at the ends of the test specimen controlled the gap width between the cartridge and the cover plate that the seals sealed against (Figs. 7b and 7c). Blocks of different thicknesses were used to vary the gap width. A small amount of room temperature vulcanized silicone (RTV) was placed between the spacer blocks, filler blocks, and the cartridge to prevent flow from passing through these gaps. Another O-ring was placed in a groove on the surface of the test fixture and into a groove in the spacer blocks to seal the plenum chamber upstream of the test seal. For the tests performed on the shorter 6.5-in. seals, grooves in the filler blocks on either side of the seal specimen extended the O-ring path from the spacer blocks to the ends of the seal specimen (Fig. 7c). For both seal lengths, the ends of this O-ring were pressed up against the ends of the test seal to prevent flow from passing around the ends of the seal. For the 12-in. seals, end effect leakage was minimized by exposing only the center 10 in. of the seal to the prescribed gap. To reduce the effects of flow passing between the seal ends and the O-ring, 1 in. at each end of the 12-in. test specimen was embedded into the fixture to produce a gap width of zero in these areas. The ends of the 6.5-in. test seals were coated

with RTV to form a better seal between the seal ends and the O-ring to minimize end effects. Preload was applied to the test seal through an interference fit between the seal and the cover plate.

#### Test Matrix/Nonscrubbed Seals

A series of flow tests was conducted using 12-in. seal specimens. Single-seal flow tests were conducted on nonscrubbed seals at compression levels of 0, 10, 20, and 25% of the specimen's overall diameter. Double-seal flow tests were conducted on as-received seals at 0, 10, and 20% compression. The 12-in. seals were not coated with vermiculite, whereas the 6.5-in. seals were coated for the scrub tests.

#### Test Matrix/Scrubbed Seals

Flow tests were performed at 20% compression on the 6.5-in. double seals that were attached to carrier plates. Tests were performed on two 6.5-in. segments that were cut out of the 27.5-in. seal that was used in the first scrub test. One segment was chosen from an area with the worst amount of wear, whereas the other segment was selected as the area with the least amount of damage. Flow tests were also done on the seal specimen from the second scrub test that had been scrubbed against the tile joint that was covered with Kapton tape. Additional tests were performed on a baseline nonscrubbed double seal attached to a carrier plate to determine the effects of scrubbing and carrier plate attachment on seal flow rates.

To simulate conditions in which a gap filler had fallen out of the joint between adjacent tiles on the sealing surface, flow tests were performed in which a groove was cut into the cover plate. This 0.050 in. wide by 0.060 in. deep groove simulated a gap between the tiles through which air could flow past the seals. Tests were performed using the worst-worn seal segment from the scrub tests and the nonscrubbed seal segment sealing against this grooved cover plate.

To determine the best possible flow rates through these seals, tests were performed in which RTV was placed in between a seal and carrier plate and on the backside of the carrier plate to eliminate these leak paths around the seal. The seal used for these tests was the least damaged segment that was cut out of 27.5-in. scrub tested seal. These tests were performed against the flat cover plate.

All flow tests were performed with a 0.25-in. seal gap. Both primary and repeat flow tests were conducted for all of the given test conditions.

### Arcjet Tests

#### Test Facility

A series of tests were performed on the 6-pcf seal design in the 20 Megawatt Panel Test Facility at NASA Ames Research Center to simulate exposure of the seals to the extreme thermal conditions that they would experience during atmospheric reentry. The seals were installed in a test fixture that was positioned in the test chamber such that high-temperature exhaust flow passed out of the semi-elliptical nozzle (17-in.-wide nozzle) of the arcjet heater and over the top surface of the test fixture. A gap in the test fixture allowed hot air to flow down to the seals. During testing, the test chamber was evacuated down to a pressure of  $5 \times 10^{-2}$  torr ( $9.67 \times 10^{-4}$  psi) to

draw flow out of the arcjet nozzle, over the test article, and through the seals. The arcjet facility has the capability of producing heat fluxes on the order of 0.5–75 Btu/ft<sup>2</sup> s with temperatures on the top of the test article as high as 2200°F (Ref. 7).

#### Test Fixture

The test fixture was based on the geometry of the X-38 body flap but had many similarities to the rudder/fin hinge-line seal configuration (Fig. 8). It consisted of a stationary upstream structure and a movable control surface. Test seals were placed into the gap along the hinge line between the stationary structure and the control surface. The depth of the gap from the freestream to the seal of 1.5 in. was in the range of the depths from the freestream to the rudder/fin hinge-line seal, depending on rudder position. The 0.25-in. seal gap size is used in both the X-38 rudder/fin and body flap sealing applications. The seals were installed in the test fixture so that they were under 20% compression for these tests. The control surface could be actuated over a range of 0–10 deg with respect to the stationary surface, and the table upon which the test fixture sat could be adjusted to vary the angle of attack of the entire test fixture over a range from –4 deg (out of the flow) to +6 deg (into the flow). The greatest angle that the control surface was raised into the arcjet flow equaled the sum of both angles, for example, 6-deg table angle plus 10-deg control surface angle is equal to 16-deg control surface deflection into flow. Raising the control surface into the arcjet flow raised the static pressure above the sealed hinge line, deflected high-temperature flow into the seal gap, and increased seal and gap temperatures.

The test fixture was composed of a water-cooled copper box and a movable stainless steel control surface section that were covered with AETB-8 tiles to simulate the rudder/fin thermal protection system in the X-38. For each test a single 19-in.-long seal was used with a "tail" of Nextel fabric sewn on to it. This tail was clamped in between tiles in the stationary structure of the test fixture to secure the seal in place (Fig. 8). The test fixture was instrumented with 34 thermocouples and 7 pressure taps to record temperatures and pressures upstream and downstream of the test specimens and monitor the health of the test fixture. A more detailed description of the test fixture, instrumentation, and procedure used to perform these tests can be found in the final report by Newquist et al.<sup>8</sup>

## Results and Discussion

### Temperature Exposure Test Results

The temperature exposure tests conducted on the seals caused a distinct change in their shape and properties. After temperature exposure at 1900°F for 7 min while compressed between two steel plates, the seal specimens did not return to their original circular cross section. They took on an elliptical cross section that was quite flat in the areas that were in contact with the plates (Fig. 9). The specimens were stiffer and much less flexible than they were before the temperature exposure.

Most of these changes are believed to be due to changes that occurred in the Inconel X-750 spring tube. The Inconel X-750 spring tube contributes significantly to the resiliency of the seals and appeared to have taken on a large permanent set during these tests. This is because the yield strength of Inconel X-750 at 1900°F is less than

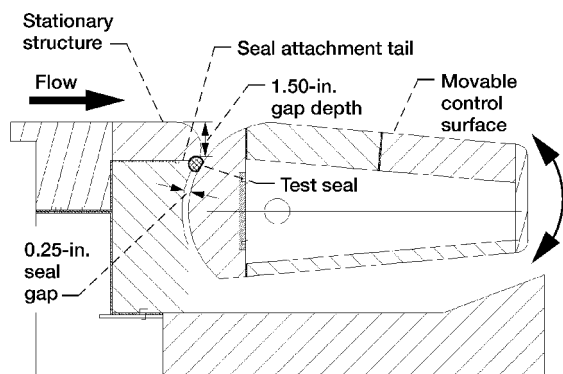


Fig. 8 Cross section of arcjet test fixture.

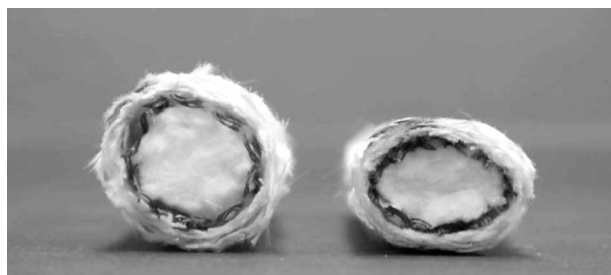


Fig. 9 Photograph of 6-pcf X-38 seals before (left) and after (right) 1900°F temperature exposure.

**Table 2** X-38 6-pcf seal residual interference, contact width, unit load, preload, and stiffness for several linear crush conditions<sup>a</sup>

Nominal linear crush, %	Linear crush, in.	Residual interference (springback), in.	Contact width, in.	Unit load, lbf/in.	Preload, psi	Stiffness $k$ at % linear crush, <sup>b</sup> lbf/in.
<i>As received</i>						
10	0.062	0.046	0.330	0.54	1.7	14
20	0.124	0.084	0.455	2.01	4.4	39
25	0.155	0.115	0.581	2.98	5.1	51
30	0.186	0.118	0.692	4.47	6.4	66
<i>After 1900° F exposure</i>						
20	0.124	0.018	0.379	0.91	2.4	58
25	0.155	0.036	0.452	1.77	3.9	76
30	0.186	0.029	0.489	1.90	3.9	106

<sup>a</sup>Diameter 0.620 in.<sup>b</sup>Seal stiffness is calculated as the slope through the final two data points at the maximum amount of compression.

5% of its room-temperature strength.<sup>9</sup> This prevented the seal from returning to its original circular cross section and caused it to take on the new elliptical cross section. The Nextel 312 ceramic fabric that formed the outermost layers of the seals and the Saffil batting in the seal core did not undergo any noticeable changes during these tests. Further discussions of the specific changes to seal resiliency and stiffness due to 1900° F exposure will be addressed in the following sections.

#### Porosity Measurement Results

Porosity measurements were made on four specimens of the 6-pcf seal design using the Archimedes approach. The porosity values measured for these specimens ranged from 83.3 to 85.2% with an average porosity of 84.4%. This means that almost 85% of the volume of the seal was composed of air and only 15% was actual material. This value was corroborated by making porosity measurements on two additional specimens using the mass/volume approach. The porosity values for these two specimens were 81.3 and 82.6% for an average porosity of 82%. The mass/volume porosity measurement was done in a compressed state that could account in part for the slightly lower measured porosity.

The high seal porosity level is attributed primarily to the loose packing of the 6-pcf Saffil batting. For comparison purposes, thermal barriers braided from continuous fibers have porosities in the range of 37–50% (Ref. 10). Porosity is important for understanding the thermal and flow response characteristics of these seals and is an important variable used in seal thermal analyses.

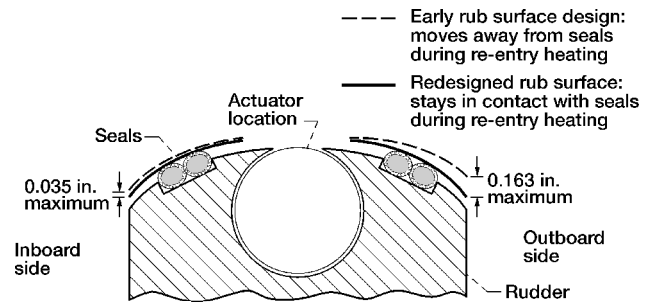
#### Compression Test Results

Table 2 is a summary of the results of the compression tests performed on the 6-pcf seal design in the as-received condition and after 1900° F temperature exposure. Values listed in Table 2 are for single seals and include the measured residual interference, contact width, unit load, preload, and seal stiffness per unit inch of seal for each amount of linear compression at which the tests were performed.

#### Residual Interference/Resiliency

The residual interference, or springback, of the seals generally increased as percent linear compression increased (Table 2). However, exposure of the seals in a compressed state at 1900° F for 7 min caused a large permanent set and loss of resiliency. At each compression level, the residual interference, or springback, of the temperature-exposed seals was only 20–30% of that for the as-received seals. As already discussed, most of this loss of resiliency is believed to be due to permanent set that occurred in the Inconel X-750 spring tube during temperature-exposure testing. In the as-received seal, the spring tube contributes significantly to the resiliency of the seals.

The main requirement for the X-38 rudder/fin seals, and control surface seals in general, is that they remain in contact with the sealing surface while the vehicle goes through the maximum reentry heating cycle. Good seal contact is required to prevent hot gases from leaking past the seals and into cavities behind them in which

**Fig. 10** Schematic of X-38 rudder/fin cross section showing vertical Inconel rub surface redesigned to accommodate lack of seal resiliency (not drawn to scale).

low-temperature structures reside. An additional requirement is that the seals are able to accommodate differences in thermal expansion between parts adjacent to them that cause the seal gap to change size. Because these seals experienced a large permanent set and loss of resiliency during temperature exposure, designers were forced to change the X-38 rudder/fin vertical rub surface design to ensure that the seals remained in contact with the sealing surface during reentry. Finite element analyses were performed to determine how different Inconel rub surface designs would deform and deflect under anticipated mechanical and thermal loads during flight. Different rub surface thicknesses, constraint schemes, and attachment methods were evaluated. Early designs yielded rub surfaces that moved away from the seals such that they were not in contact with the seals during maximum heating conditions (Fig. 10). Some locations on the rub surface moved as much as 0.163 in. away from the seals on the outboard side of the rudder/fin. After several iterations, a final Inconel rub surface design was selected that was 0.05 in. thick with gussets distributed on its outboard side to restrict deflection based on the predicted temperature distribution. This design provided engagement between the seals and the rub surface during maximum heating conditions (Fig. 10).

#### Unit Load (Load per Unit Inch)/Preload/Seal Stiffness

The amount of unit load (or load per unit inch), seal preload (or footprint contact pressure), and seal stiffness per unit inch of seal increased as the amount of linear crush was increased on both the as-received and temperature-exposed seals (Table 2). Although the temperature-exposed seals were noticeably stiffer and less flexible to the touch than the as-received seals, unit loads and preloads were lower for the temperature-exposed seals. These results can be explained by the differences in stiffness between seals in the two conditions. Seal stiffness per unit inch of seal was calculated as the slope through the final two data points on a load vs compression plot at the maximum amount of compression.<sup>3</sup> Seal stiffness after 1900° F exposure was 1.5 times higher than for the as-received seals at 20% compression. Therefore, even though unit loads and preloads were lower for the temperature-exposed seals, they were stiffer than the as-received seals at the same amount of compression. This



increased stiffness is again believed to be due to changes that occurred to the Inconel X-750 spring tube during the 1900°F exposure.

Sealing surfaces that control surface seals mate against include shuttle-type thermal tiles, ceramic matrix composite structures, and metallic structures. Of these surfaces, shuttle thermal tiles are the most damage prone in terms of the unit loads that they are able to resist. In the X-38 rudder/fin seal application, for instance, the seals should not put a load of more than 5 lb/in. of seal on the thermal tiles that make up the sealing surfaces. For this application, the seals are to be installed at approximately 20% compression with a nominal 0.25-in. gap between the surfaces of the rudder and fin. The results in Table 2 show that unit loads were below 5 lb/in. of seal for all compression levels tested. The maximum seal preload, or contact pressure, that was measured was 6.4 psi for the as-received seal at 30% compression. Even at this high level of compression, the pressure that would be applied to the tiles would be seven times lower than the flatwise tensile strength of 46 psi for the tiles and nine times lower than the compression strength.<sup>3</sup> The results of these compression tests indicate that the 6-pcf seals meet the seal load requirements established for the X-38 rudder/fin seal application.

### Scrub/Wear Test Results

In the first scrub test, the 27.5-in. seal was scrubbed for 1000 cycles over the three RCG/TUFI coated AETB-8 tile rub surfaces. After the test, there were several areas of the seal that were clearly more damaged than other areas. At seal locations approximately 8, 17, and 21 in. from the pivot point of the test fixture, the outer Nextel sheath layers were so worn away that the Inconel spring tube was exposed. Figures 11a and 11b show these worn areas of the seal. Away from these specific locations, the seal was in much better condition. The outer Nextel sheath layers showed signs of wear and some fiber breakage, but they were still intact. After 1000 scrub cycles, broken Nextel fibers were spread over the area in which the seals were swept over the tiles, but the tile surfaces were still in good condition. There was some minor wear along one tile edge 17 in. from the pivot point.

The major cause of seal wear and degradation in this test was roughness associated with the joints between adjacent tiles. The

seal locations that were more heavily damaged at 8 and 17 in. from the test fixture pivot corresponded to locations of joints between tiles. Three tiles were used to form the rub surface, and gap fillers were stuffed into the joints between the tiles. The gap fillers were installed flush with the outer surface of the tiles as they would be in a vehicle to minimize sneak flows between adjacent tiles above the gap fillers. To make the tiles smoother than they were in their as-fabricated condition, the tiles were sanded by hand to a surface roughness of 80–90  $\mu$  in. rms. The process of hand sanding the tiles produced very smooth surfaces in the centers of the tiles but left the tile edge surfaces slightly rougher. The rougher tile edges and the gap fillers combined to wear away the outer Nextel sheath layers of the seal during the 1000 cycle scrub test. Areas of the seal away from tile joints showed only superficial Nextel fiber damage.

Based on the results of the first scrub test, a second test was performed in which a 6.5-in. seal specimen was scrubbed over an area of the rub surface in which the joint between two tiles was covered with a layer of Kapton tape. This was done to remove the tile edges and gap fillers as sources of roughness for seal degradation. The condition of this seal after 1000 scrub cycles is shown in Fig. 11c. The seal showed few signs of damage with the Nextel sheath layers remaining intact throughout the test. Clearly, the Kapton tape was very effective in reducing seal degradation at a tile intersection. The tape was evaluated in this study as a means of mitigating seal damage during considerable preflight cycling of the rudders and seals for checkout purposes. It is recognized that the tape would not survive reentry temperatures.

Another test goal was to evaluate how well the seals were able to move off of and then reengage the edge of the tile rub surface. This movement is a unique feature of the X-38 rudder/fin seal application in that control surface seals generally remain in contact with their sealing surface during use. Observation during both scrub tests revealed that the seals were able to disengage and reengage the edges of the tiles satisfactorily. They remained securely attached to the movable arm, qualifying the Inconel wire attachment technique. The amount of torque required to disengage and reengage the seals was recorded periodically during each test. These torque measurements are shown in Fig. 12. For both seals, the amount of torque

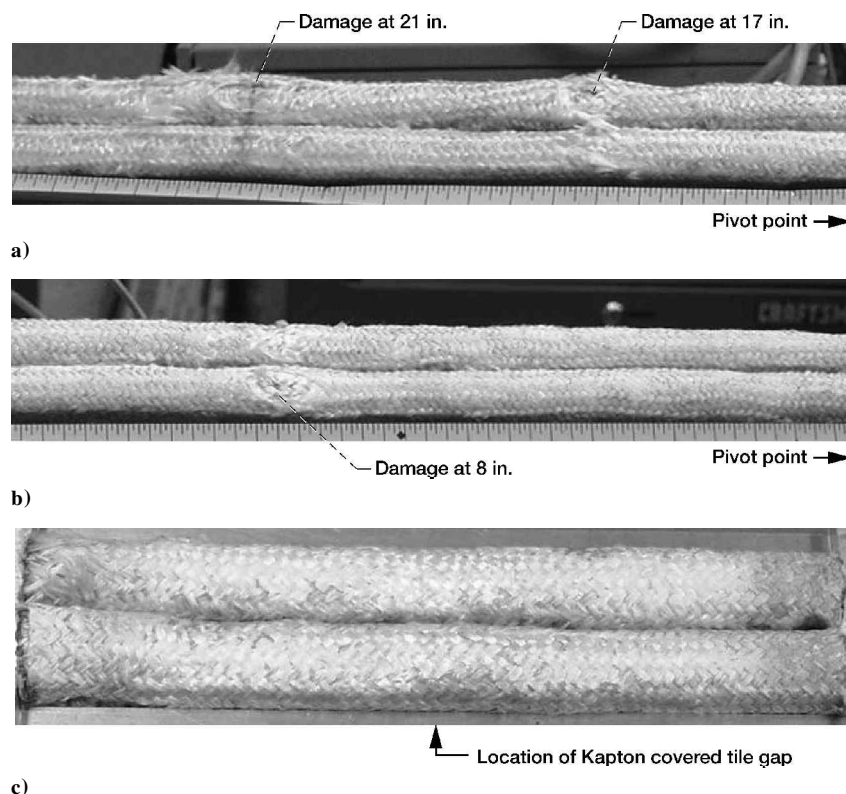


**Fig. 11** Photographs of seals after 1000 scrub cycles against RCG/TUFI-coated AETB-8 rub surface: a) 27.5-in. seal with damage indicated at locations 17 and 21 in. from pivot of scrub test fixture, b) 27.5-in. seal with damage indicated at location 8 in. from pivot of test fixture, and c) 6.5-in. seal with minimal damage after scrubbing against tiles with Kapton tape covering gap between adjacent tiles.

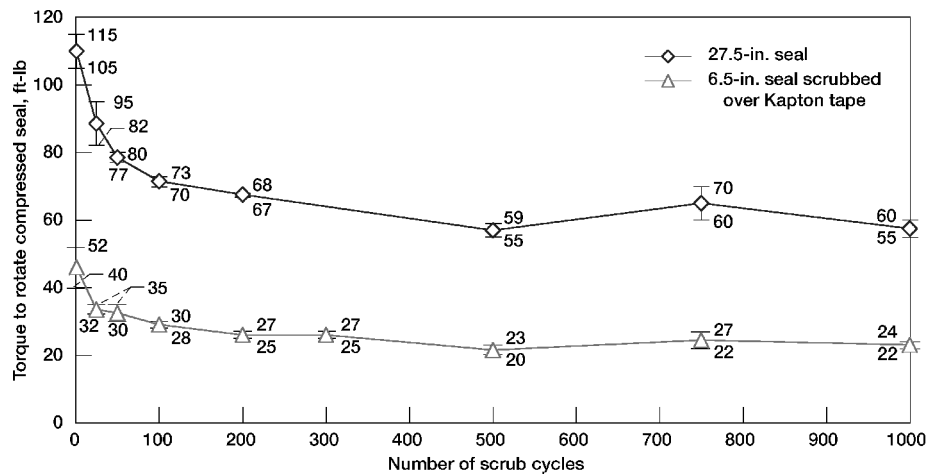


Fig. 12 Torque results for scrub tests of seals against RCG/TUFI-coated AETB-8 rub surface; range and midpoint of torque values shown for a given scrub cycle.

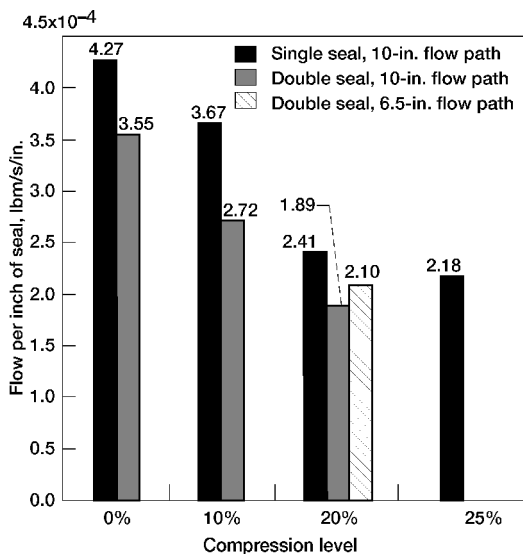


Fig. 13 Effect of number of seals, compression level, and seal length on seal flow; seals are in as-received condition (nonscrubbed),  $\Delta P = 56$  psf, and gap = 0.25 in.

needed to disengage and reengage the seals dropped off after the first cycle, leveled off at about half of the initial torque value around the 100th cycle, and remained relatively constant for the remainder of the 1000 scrub cycles. The drop in torque over the first 100 cycles was caused by the seals settling into the groove into which they were installed and experiencing some wear. This reduction in torque with cycling is beneficial in that it puts less stress on the rub surface tiles over time. The measured peak torque of 115 ft · lb is less than 13% of the rated actuator torque of 875 ft · lb (at a rotation speed of 30 deg/s) ensuring that the X-38 rudders can be actuated with the seals installed.

Results of these tests also showed that reducing the roughness of the sealing surface by sanding the tiles and covering joints between tiles enabled the seal to endure a 1000-cycle scrub test. Similar tests in which the same seal design was scrubbed against unsanded tiles revealed significant damage to the seals after only 100 scrub cycles.<sup>6</sup> For applications in which this type of seal would be required to withstand 1000 or more scrub cycles over multiple missions, making the seal rub surface as smooth and continuous as possible is critical.

#### Flow Test Results

Seal flow rates are summarized in Figs. 13 and 14. Figure 13 presents flow rates at compression levels of 0, 10, 20, and 25% for both single and double seals that had not been scrub tested. Figure 14

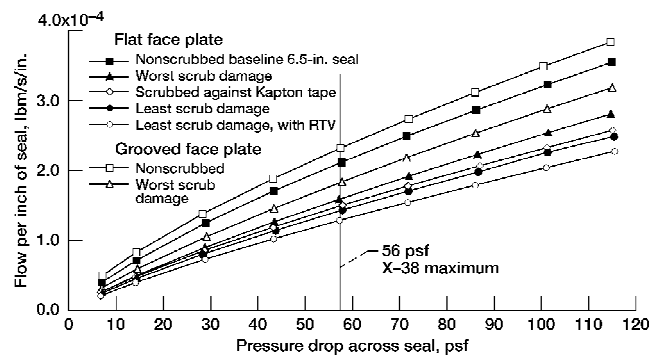


Fig. 14 Flow vs pressure data for 6.5-in. double seals at 20% compression under different test conditions with a gap of 0.25 in.

shows flow vs pressure curves for the variety of test conditions at which the 6.5-in. double seals were tested. The flow rates shown in Figs. 13 and 14 are presented as the measured flow rate at room temperature divided by the length of seal exposed to flow in the test fixture (either 6.5 or 10 in.).

#### Effect of Compression Level

As shown by the flow results in Fig. 13, flow rates decreased with higher compression levels. As the amount of compression on the seals was increased from 0 to 25% the amount of flow through the seals decreased. This is to be expected because the act of compressing these seals closed the gaps and flowpaths in their porous structures and allowed less flow to pass through them. Note in Fig. 13 that the flow for a double seal at 0% compression was nearly twice that for a double seal at 20% compression. Flow rates measured at 0% compression represent seals in an unloaded condition.

#### Effect of Single vs Double Seals

Flow rates through a double-seal configuration were lower than those for a single seal at 0, 10, and 20% compression (Fig. 13). Adding a second seal into the flowpath reduced flow through the seals by roughly 17–26% as compared to flow rates through single seals at the same compression level. Although the second seal caused a drop in flow rates, it did not cut the flow in half. This type of behavior in multiple-seal flow tests was observed previously by Steinetz and Adams,<sup>5</sup> and will be discussed further in the section on seal permeability.

Note also that the flow rate for the 6.5-in. double seal was about 10% higher than the flow rate through the 12-in. seal (with a 10-in. flow path) at the same compression level. This result could be due partly to end effects for the 6.5-in. seals that were not present for the longer seals. As already discussed, the 12-in. seals were installed such that 1 in. at each end of the seal was embedded into the fixture

to reduce the effects of flow passing between the seal ends and the O-ring. Because the 6.5-in. seals were installed in the center of the 10-in. flowpath, the butt joint between the seal ends and the O-ring was in the flowpath. Another possible reason for the higher flow rate through the 6.5-in. seals was that these seals were mechanically attached to a carrier plate, whereas the 12-in. seals were installed as-is into the seal cartridge. The shorter seals could have incurred some minor damage in the process of attaching them to the carrier plate that could have led to slightly higher flow rates. It is also possible that the vermiculite coating on the 6.5-in. seals reduced the compliance of the outer Nextel sheath and led to higher flow rates.

#### Effect of Scrubbing

Figure 14 presents flow results for the 6.5-in. seals in both nonscrubbed- and scrub-tested conditions. Flow rates through each of the scrubbed seal specimens were actually lower than the flow rates through the nonscrubbed seal. This type of behavior has been observed before by Steinetz et al.<sup>11</sup> Flow rates decreased after scrub cycling most likely because the seals and the nature of the braid surface compacted during scrub testing.

Of the seal specimens that were scrub tested, the segment of the 27.5-in. scrub-tested seal with the worst damage had the highest flow rates, whereas the segment of that seal with the least scrub damage had the lowest flow rates. The seal segment with the worst damage most likely had the highest flow rates out of the scrubbed seals because its outer sheath layers were quite damaged. This seal segment included both of the damaged areas shown in Fig. 11a in which the seal sheath was worn away so that the Inconel spring tube was showing. These damaged areas likely allowed more flow to pass through the interface between the seal surface and the surface of the cover plate, resulting in higher flow rates. The seal that was scrubbed over the tile joint with the Kapton tape over it had flow rates that were only slightly higher than those for the least damaged segment of the 27.5-in. scrub-tested seal. For example, the flow rate through the seal scrubbed against Kapton tape was only 5% higher than the flow rate for the least damaged seal at 56 psf (Fig. 14). This difference in flow rates is basically negligible given that both seal specimens showed little wear after 1000 scrub cycles.

The results of these tests show that some amount of seal scrubbing while under compression actually improves the flow resistance of these seals. This drop in flow rates through scrubbed seals occurs until the seals reach a point at which they become overly damaged. At this point, the damaged areas of the seal cause seal flow rates to increase.

#### Effect of Groove in Cover Plate

To simulate flow conditions in which a gap filler had fallen out of the joint between adjacent tiles on the sealing surface, flow tests were performed in which a 0.050 in. wide by 0.060 in. deep groove was cut into the cover plate. Tests were performed on both the worst-worn seal segment from the scrub tests and on the nonscrubbed seals. Flow rates using the grooved cover plate increased for both seals as compared to flow rates using the flat cover plate (Fig. 14). At a 56-psf pressure drop across the seals, flow through the nonscrubbed seal increased by more than 9%, and flow rates for the scrubbed seal increased by over 16%. These results are to be expected because the groove provided an additional flowpath through which air could flow past the seals.

#### Effect of RTV Behind Seals

A set of flow tests was performed using the flat cover plate and the least-damaged segment from the 27.5-in. scrub-tested seal in which leak paths around the backside of the seal were eliminated by placing RTV on the backside of the carrier plate and in the interface between the back of the seal and the carrier plate. As shown in Fig. 14, the flow rate for the seal with RTV behind it was reduced by over 10% at a pressure of 56 psf as compared to the flow rate through the same seal without RTV. Flow rates such as these represent a best-case condition in which the seals had been compacted but not damaged by scrub cycling and had not yet gone through a reentry heating cycle that would destroy the RTV.

#### Seal Permeability

In addition to porosity and flow rates through the seals, seal permeability is often used to represent the resistance to flow through a seal. In this study permeability was defined as follows:

$$K = (\dot{m}\mu L)/(\rho A \Delta P) \quad (3)$$

The length of the flowpath through the seal was either 0.62 in. (0.0517 ft) for a single seal or 1.30 in. (0.108 ft) for a double seal. The frontal area of the seal exposed to flow was calculated as the length of the seal exposed to flow (either 6.5 or 10 in.) multiplied by the gap size of 0.25 in. Thus, values for the frontal area were either 2.5 in.<sup>2</sup> (0.0174 ft<sup>2</sup>) for the longer seals or 1.63 in.<sup>2</sup> (0.0113 ft<sup>2</sup>) for the shorter seals. The remaining variables of flow through the seal and pressure drop across the seal came from the flow test results for each seal.

Figure 15 presents seal permeability for nonscrubbed single and double seals as a function of compression level. The permeability values plotted in Fig. 15 were determined using the flow rate for each seal at a pressure drop across the seal of about 56 psf. For both the single- and double-seal configurations, seal permeability decreased as the amount of compression on the seals increased. Because the permeability calculation is based on measured flow rates, this result is to be expected because the flow rates also decreased with increases in compression level.

Seal permeability for a double-seal configuration was higher than it was for a single seal (Fig. 15). This is due to the way that the permeability equation is defined. Permeability is a direct function of the flow through the seal and the length of the flow path through the seal. As already discussed, addition of a second seal into the flowpath reduced the amount of flow past the seals, but it did not cut the flow rate in half. Adding a second seal doubled the length of the flowpath through the seals, though. Because both of these terms are in the numerator of the permeability equation, doubling the flow path through the seal while reducing the flow rate by less than half caused an increase in permeability for the double seals as compared to the single-seal configuration.

Seal permeability values for the 6.5-in. double seals at 20% compression with a 56-psf pressure drop across the seals are presented in Table 3. These permeability values are referred to as "apparent"

**Table 3 Apparent permeability of 6.5-in. double seals at 20% compression with 56-psf pressure drop across seals**

Face plate condition	Seal condition	Permeability, ft <sup>2</sup> × 10 <sup>-9</sup>
Flat	Nonscrubbed, baseline 6.5-in. seal	1.15
Flat	Worst scrub damage	0.86
Flat	Scrubbed against Kapton tape	0.81
Flat	Least scrub damage	0.77
Flat	Least scrub damage, with RTV	0.70
Grooved	Nonscrubbed	1.26
Grooved	Worst scrub damage	0.99

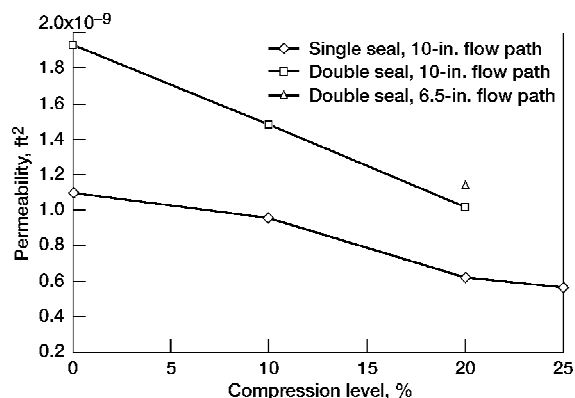


**Fig. 15 Seal permeability vs compression level for nonscrubbed single and double seals.**

permeability because the flow rates used in these calculations were a function of the test conditions. For example, flow tests were performed using a grooved cover plate that allowed air to flow around the seals. The flow rates measured in those tests were a function of both flow through the seals and flow around the seals. The permeability values shown in Table 3 assumed the same ranking as the flow rates plotted in Fig. 14 such that the seal with the highest flow rates also had the highest permeability. This result is to be expected because the permeability calculation is based on the measured flow rates.

### Arcjet Test Results

The data presented in this section are sample data from a series of 12 test runs performed on several different seal designs under a variety of test conditions. Details of the complete test program funded by NASA Glenn are in a final report by Newquist et al.<sup>8</sup>

#### Open Gap Test

The results of an arcjet test performed with no seal installed in the test fixture are shown in Fig. 16. This test (test 12 in the series) served as a baseline to determine how hot the open gap in the fixture would get with no seal installed. The open gap was designed to be nominally 0.25 in. wide but ended up ranging from 0.288 in. at a control surface angle of 0 deg to 0.260 in. at 10 deg. The test was performed with the overall test fixture (table) angled up into the arcjet flow at a 6-deg angle. The control surface was initially fixed at its baseline 0-deg position when the test started, and it was held there until the top surface temperature stabilized at about 2200°F. The control surface was held at 0 deg for 39 s under these maximum heating conditions and was then rotated upward into the stream an additional 2 deg and held in that position for the remainder of the test.

When the 6-deg angle of the overall test fixture was included, the control surface total angle into the flow was 8 deg. After 23 s in this configuration, portions of the test fixture reached their temperature limit, and the test was ended.

Figure 16 shows that the temperature inside the seal gap at a position 0.5 in. above the usual seal location reached 2230°F while the control surface was at its 0-deg position and peaked at 2240°F at the 2-deg position. The gap temperature 0.5 in. below the seal would have been located reached 2010°F at the 0-deg control surface position and 2100°F by the end of the 62-s test at the 2-deg control surface angle. Although no seal was installed in the gap for this test, the temperature drop across the seal location can be evaluated as the difference between the temperatures recorded 0.5 in. above and below where the seal would have been. Before the control surface was rotated, the temperature drop across the seal location was about 220°F. After the control surface was rotated, the temperature drop decreased to 140°F by the end of the test. The temperature 1.5 in. below the seal position rose to 1620°F by the end of the test. These results confirm that a seal is required in the X-38 rudder/fin gap and in control surface gaps in general to reduce heat fluxes into the gap and protect underlying structures. The study by Wong and Kremer<sup>1</sup> also predicted high temperatures in an open rudder/fin gap and emphasized the need for a seal in the gap.

#### Arcjet Test with Seal Installed

Figure 17 shows the results of an arcjet test (test 5 in the series) with a seal installed in the gap. The 6-pcf seal was installed at 20% compression in a nominal 0.25-in. gap. As in the open-gap test, this test was performed with the overall test fixture (table) rotated up into the arcjet flow at a 6-deg angle. The control surface was again fixed at its baseline 0-deg position when the test began and held there until the top surface temperature reached a steady-state

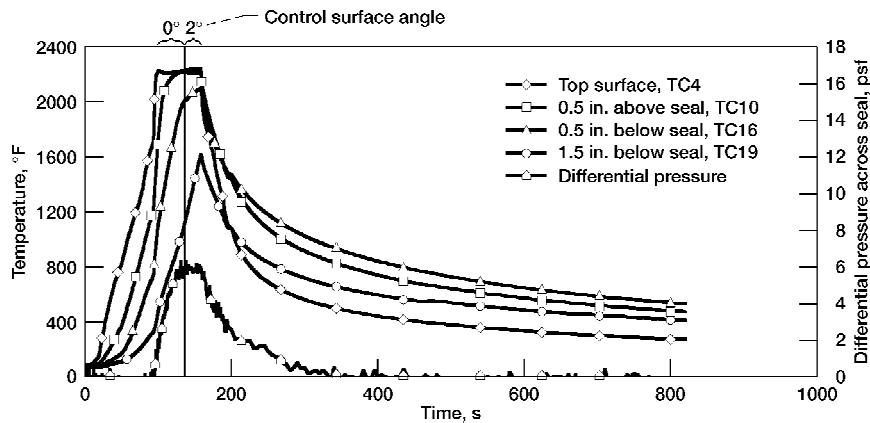


Fig. 16 Temperatures and pressure differential measured during arcjet test with no seal installed (test 12), 6-deg table angle, 0- and 2-deg control surface angles, and 0.25-in. nominal gap (symbols for identification only; data recorded every 1 s).

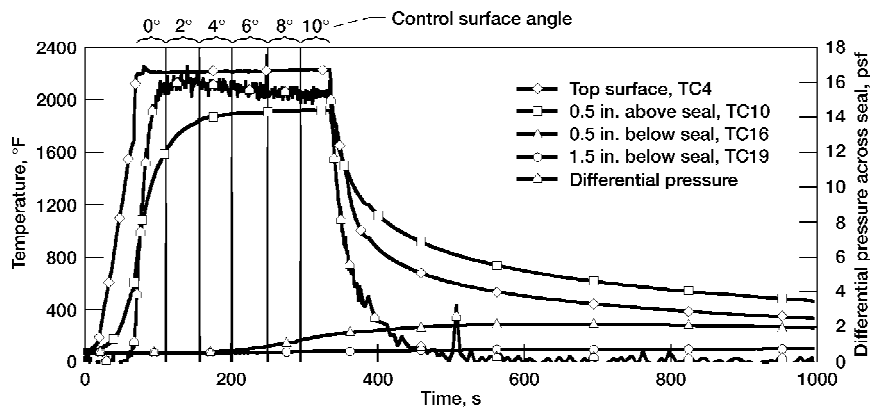


Fig. 17 Temperatures and pressure differential measured for arcjet test with seal installed at 20% compression (test 5), 6-deg table angle, 0-, 2-, 4-, 6-, 8-, and 10-deg control surface angles, and 0.25-in. nominal gap (symbols for identification only; data recorded every 1 s).

temperature condition of about 2200°F. The control surface was held at 0 deg for 38 s and then rotated upward in 2-deg increments approximately every 45 s until it was angled 10 deg with respect to the upstream stationary portion of the test fixture. It was held in this final position for an additional 41 s before the test was ended. When the 6-deg table angle was included, the final control surface position was rotated upward 16 deg into the arcjet flow. The total time spent at maximum heating conditions (2200°F on the top surface) was 263 s. This is comparable to the 250 s of peak heating for the rudder/fin seals predicted between 1100 and 1350 s of the X-38 reentry mission (Fig. 3). During the arcjet test, the average pressure differential across the seal during maximum heating conditions was 15.6 psf, indicating that flow passed through the seal (Fig. 17). This pressure level was about 44% of the 35-psf pressure predicted at the 1200-s maximum heating point during X-38 vehicle reentry (Fig. 3).

The average temperature on the top surface of the test fixture during maximum heating conditions was 2220°F. With a seal installed in the gap, the temperature 0.5 in. above the seal reached 1610°F for a 0-deg control surface angle with the table angle at 6 deg. The temperature 0.5 in. above the seal reached 1920°F by the end of the test with the control surface at 10 deg and a 6-deg table angle. Clearly, installing a seal in the gap created a flow block that limited the amount of heat convected into the gap under these extreme test conditions.

#### *Temperature Drop Across Seal*

Temperatures recorded 0.5 in. below the installed seal were much lower than those recorded in the open-gap test. During maximum heating conditions, the peak temperature only reached 207°F, resulting in a temperature drop across the seal of about 1710°F (Fig. 17). Temperatures recorded 1.5 in. below the installed seal barely increased during this test, reaching a peak temperature of 101°F. Installing a seal in the gap reduced gas temperatures to a level at which an electromechanical actuator behind the seal would survive reentry.

The seal specimen that was used for this test survived the arcjet exposure. A limited amount of damage was caused to the outer Nextel sheath layers of the seal due to limited actuation (less than 10 cycles) of the control surface during the test. Some broken fibers were seen spread over the surface of the control surface in areas where the seal was wiped over the surface, but the seal was generally in good condition after the test.

It is clear from the results of these tests that installation of a seal in the gap of the test fixture caused a large temperature and pressure drop across the seal location as compared to an open-gap condition. The seal acted as an effective thermal barrier limiting heat fluxes through the seal gap and minimizing temperature increases downstream of the seal during maximum heating conditions. The pressure differential measured across the seal was 44% of the 35-psf maximum pressure predicted at the 1200-s maximum heating point during X-38 vehicle reentry (Fig. 3). Larger pressure drops during reentry could potentially cause more flow through the seal with higher temperatures downstream of the seal. However, only one seal was used in these tests, whereas two seals will be installed side-by-side in the X-38 rudder/fin seal application. This will drop the amount of flow through the gap as shown by the results of the flow tests presented earlier.

### **Seal Requirements for X-38 vs Future Reusable Reentry Vehicles**

Seal requirements for the X-38 vehicle are different from those of future reusable reentry vehicles in several ways. The most obvious difference is that the X-38 seals are expected to be replaced after each mission, whereas seals for future reusable reentry vehicles would be required to last for hundreds of missions. Reusable seals will need to be wear resistant to endure many scrub cycles against sealing surfaces to allow for multiple missions without being replaced. They will also need to be resilient after repeated temperature exposures.

Control surface seals for the X-38 are expected to be used at much higher temperatures (1900°F) than similar seals that are used as elevon and body flap seals on the space shuttle. These shuttle seals are generally used at temperatures less than 1500°F. Seals for

future reusable reentry vehicles will likely be placed closer to the vehicle surface and closer to the extremely hot gases that pass over the outside of the vehicle during reentry. Thus, future control surface seals will need to endure temperatures similar to those predicted for the X-38 seals, if not higher. The seal designs in this study took on a large permanent set after one temperature exposure due mostly to permanent deformation of the Inconel X-750 spring tube. This loss of resiliency after temperature exposure most likely would not be acceptable for reusable applications. Most metals cannot endure the high temperatures that the seals will experience in high-temperature applications without causing the seals to lose resiliency. For future applications the seals will most likely have to be composed entirely of ceramic components. Preloading devices can also be placed behind the seals to improve resiliency. Requirements for higher temperatures and reusability in future reentry vehicles will necessitate that novel seal designs are developed that exhibit low flow rates and remain resilient and wear resistant for multiple missions.

### **Conclusions**

Reentry vehicles generally require control surfaces such as rudders, body flaps, and elevons to steer or guide them during reentry. Control surface seals are installed between these movable surfaces and stationary portions of the vehicle both along hinge lines and in areas where control surface edges seal against the vehicle body. These seals must operate at high temperatures and limit hot-gas ingestion and transfer of heat to underlying low-temperature structures to prevent overtemperature of these structures and possible loss of vehicle structural integrity. The main objective of this study was to evaluate a currently available control surface seal design for applications in future reentry vehicles based on the design requirements of the X-38 rudder/fin seal system as a case study.

The baseline seal examined in this study was a thermal barrier used in several locations on the space shuttle. A thermal analysis of the rudder/fin seal assembly based on representative heating rates predicted a peak seal temperature of 1900°F. Seals were heated in a compressed state at this peak temperature to evaluate the effects of temperature exposure. Room-temperature compression tests were performed to determine load vs linear compression, preload, contact area, stiffness, and resiliency characteristics for as-received and temperature-exposed seals. Seal scrub tests were performed to examine durability and wear resistance and to recommend surface treatments required to maximize seal wear life. Flow tests were conducted at ambient temperature to examine seal leakage characteristics both before and after scrubbing. Arcjet tests were performed to determine experimentally anticipated seal temperatures for representative flow boundary conditions (pressures and temperatures) under simulated vehicle reentry conditions. Based on the results of these tests, the following conclusions are made:

- 1) Exposure of the seals in a compressed state in a tube furnace at 1900°F for 7 min resulted in permanent set and loss of seal resiliency presumably due to yielding of the Inconel X-750 spring tube. This loss of seal resiliency was accounted for in the redesign of the vertical Inconel rudder/fin rub surface. The redesigned Inconel rub surface was made stiffer to limit thermally induced movements away from the seals so that seal contact would be maintained. From a resiliency standpoint, the double seal should follow the Inconel rub surface for a single use but should be replaced before subsequent flights.

- 2) Unit loads and contact pressures for the as-received 6-pcf seal were below the 5-lb/in. and 10-psi shuttle thermal tile limits for all compression levels that were tested.

- 3) The seals survived a 1000 cycle ambient-temperature scrub test against sanded RCG/TUFI coated AETB-8 tile surfaces. They were able to disengage and reengage the edges of the rub surface tiles while remaining securely attached to their carrier plate, thereby qualifying the Inconel wire mechanical attachment method. Furthermore, the seals did not damage the shuttle tiles that they were scrubbed against. Finally, making the seal rub surface as smooth and continuous as possible greatly improved seal wear resistance.

- 4) Arcjet test results confirmed the need for seals in the rudder/fin gap location. Installation of a single seal in the gap of the test fixture

caused a large temperature drop (1710°F) across the seal. The seal acted as an effective thermal barrier to limit heat convection through the seal gap and minimize temperature increases downstream of the seal, for example, to the actuator cavity, to acceptable (< 200°F) levels.

The results of these tests have verified that this seal is satisfactory for the X-38 application. However, requirements for higher temperature limits and 100–1000 cycle reusability in future reusable launch vehicles necessitate the development of high-temperature seal designs that remain resilient for multiple missions while still exhibiting low flow rates and good wear resistance.

### Acknowledgments

The authors gratefully acknowledge Jeff Hagen and Prakash Chaudha (Lockheed Martin Space Operations) for their contributions in designing the scrub test fixture; Larry Zielke (NASA Johnson Space Center) for his assistance in conducting the scrub tests; Ron Lewis and Winston Goodrich (NASA Johnson Space Center) and Ignacio Norman (The Boeing Company) for their work on the heat transfer analyses; and Tom Doeberling (NASA John H. Glenn Research Center) and Dick Tashjian (QSS) for their assistance in test support.

### References

- <sup>1</sup>Wong, H., and Kremer, F., "Numerical Assessment on the Heating of the Rudder/Fin Gap in X-38 Space Vehicle," *3rd European Symposium on Aerothermodynamics for Space Vehicles*, SP-426, ESA, 2000, pp. 77–85.
- <sup>2</sup>Nestler, D. E., "An Engineering Analysis of Reattaching Shear Layer Heat Transfer," AIAA Paper 72-717, June 1972.
- <sup>3</sup>Dunlap, P. H., Steinetz, B. M., and Curry, D. M., "Rudder/Fin Seal Investigations for the X-38 Re-Entry Vehicle," NASA TM-210338/REV1, Nov. 2000; also AIAA Paper 2000-3508, Nov. 2000.
- <sup>4</sup>Steinetz, B. M., Adams, M. L., Bartolotta, P. A., Darolia, R., and Olsen, A., "High-Temperature Braided Rope Seals for Static Sealing Applications," *Journal of Propulsion and Power*, Vol. 13, No. 5, 1997, pp. 675–682.
- <sup>5</sup>Steinetz, B. M., and Adams, M. L., "Effects of Compression, Staging, and Braid Angle on Braided Rope Seal Performance," *Journal of Propulsion and Power*, Vol. 14, No. 6, 1998, pp. 934–940.
- <sup>6</sup>Dunlap, P. H., Steinetz, B. M., Curry, D. M., Newquist, C. W., and Verzemnieks, J., "Further Investigations of Control Surface Seals for the X-38 Re-Entry Vehicle," NASA TM-210980, July 2001; also AIAA Paper 2001-3628, July 2001.
- <sup>7</sup>Newquist, C. W., Verzemnieks, J., Keller, P. C., and Shorey, M. W., "Advanced High Temperature Structural Seals," NASA CR-210522, Nov. 2000.
- <sup>8</sup>Newquist, C. W., Verzemnieks, J., Keller, P. C., Rorabaugh, M., and Shorey, M. W., "Advanced High Temperature Structural Seals," NASA CR-211973, Oct. 2002.
- <sup>9</sup>Kattus, J. R., "Inconel X-750," *Aerospace Structural Metals Handbook*, Vol. 4, Metals and Ceramics Information Center, Battelle Labs., Columbus, OH, 1990, Article 4105, pp. 1–30.
- <sup>10</sup>Steinetz, B. M., and Dunlap, P. H., "Development of Thermal Barriers for Solid Rocket Motor Nozzle Joints," *Journal of Propulsion and Power*, Vol. 17, No. 5, 2001, pp. 1023–1034.
- <sup>11</sup>Steinetz, B. M., Kren, L. A., and Cai, Z., "High-Temperature Flow and Sliding Durability Assessments of Hypersonic Engine Seals," NASA TP-3483, Dec. 1994.

T. C. Lin  
Associate Editor